JVI Journals.ASM.org

The Multibasic Cleavage Site in H5N1 Virus Is Critical for Systemic Spread along the Olfactory and Hematogenous Routes in Ferrets

Eefje J. A. Schrauwen, Sander Herfst, Lonneke M. Leijten, Peter van Run, Theo M. Bestebroer, Martin Linster, Rogier Bodewes, Joost H. C. M. Kreijtz, Guus F. Rimmelzwaan, Albert D. M. E. Osterhaus, Ron A. M. Fouchier, Thijs Kuiken, and Debby van Riel

National Influenza Center and Department of Virology, Erasmus Medical Center, Rotterdam, The Netherlands

The route by which highly pathogenic avian influenza (HPAI) H5N1 virus spreads systemically, including the central nervous system (CNS), is largely unknown in mammals. Especially, the olfactory route, which could be a route of entry into the CNS, has not been studied in detail. Although the multibasic cleavage site (MBCS) in the hemagglutinin (HA) of HPAI H5N1 viruses is a major determinant of systemic spread in poultry, the association between the MBCS and systemic spread in mammals is less clear. Here we determined the virus distribution of HPAI H5N1 virus in ferrets in time and space—including along the olfactory route—and the role of the MBCS in systemic replication. Intranasal inoculation with wild-type H5N1 virus revealed extensive replication in the olfactory mucosa, from which it spread to the olfactory bulb and the rest of the CNS, including the cerebrospinal fluid (CSF). Virus spread to the heart, liver, pancreas, and colon was also detected, indicating hematogenous spread. Ferrets inoculated intranasally with H5N1 virus lacking an MBCS demonstrated respiratory tract infection only. In conclusion, HPAI H5N1 virus can spread systemically via two different routes, olfactory and hematogenous, in ferrets. This systemic spread was dependent on the presence of the MBCS in HA.

In wild birds and poultry throughout the world, influenza A viruses are represented by 16 hemagglutinin (HA) and 9 neuraminidase (NA) antigenic subtypes (10, 43). Influenza viruses of the H5 and H7 subtypes may become highly pathogenic avian influenza (HPAI) viruses upon transmission from wild birds to poultry. HPAI H5N1 virus, which has been enzootic in poultry for more than a decade, causes severe damage to the poultry industry. Direct transmission of HPAI H5N1 virus to humans was first detected in 1997 (7) and has continued to be reported since, causing severe and often fatal disease with a case-fatality rate of approximately 60% (44). Unlike most influenza viruses in mammals, which are normally restricted to the respiratory tract, HPAI H5N1 virus is regularly able to spread systemically in humans and other mammals (22, 33).

The highly pathogenic phenotype of avian influenza viruses in chickens is primarily determined by the acquisition of a multibasic cleavage site (MBCS) in the HA of a low-pathogenic avian influenza (LPAI) virus and is believed to be a major determinant in tissue tropism and high pathogenicity in poultry (4, 14, 20). The HA of LPAI viruses can be cleaved by trypsin-like proteases. Replication of these LPAI viruses is therefore restricted to sites in the host where these enzymes are expressed, i.e., the respiratory and intestinal tract (2). In contrast, the HA of HPAI viruses can be cleaved by ubiquitously expressed furin-like proteases, facilitating systemic replication in chickens (37).

In mammals, the association between the presence of an MBCS and systemic spread is less straightforward. None of the human pandemic or seasonal influenza viruses harbor an MBCS, and introduction of an MBCS in a human seasonal H3N2 influenza virus neither increased pathogenicity nor induced systemic spread in ferrets (34). In contrast, removal of the MBCS from HA of an HPAI H5N1 virus resulted in a virus that caused respiratory tract infection without systemic spread in mice, indicating that the MBCS is a major virulence factor for mice (12). Whether the MBCS in HPAI H5 is also a major determinant for systemic replication in other mammalian species remains unclear.

Differences in replication sites of human and avian influenza viruses in the mammalian respiratory tract correspond with differences in localization of virus attachment. In humans and ferrets, human influenza viruses attach abundantly to cells in the upper respiratory tract and along the tracheobronchial tree. In contrast, avian influenza viruses, including HPAI H5N1 virus, rarely attach to the upper respiratory tract but abundantly attach to cells of the lower respiratory tract (5, 40–42). Interestingly, HPAI H5N1 virus does replicate in the ferret nose, although it does not attach to respiratory epithelial cells of the nose (45).

Extrarespiratory tract replication of HPAI H5N1 virus has been observed—although not consistently—in humans, ferrets, mice, cats, palm civets, tigers, leopard, domestic dog, American mink, fox, and stone marten (23, 33). In ferrets, animals commonly used to study influenza virus infections, as they closely resemble humans in receptor distribution and disease signs, systemic virus replication has been reported for HPAI H5N1 viruses (11, 25) although this depends on the route of inoculation and the virus isolate used (3, 24, 36).

Several studies have shown that the central nervous system (CNS) is the most common extrarespiratory site of replication after experimental intranasal inoculation. The neurotropism of influenza viruses, including HPAI H5N1 viruses, has been studied in mice (15, 27, 28, 31, 32, 39) and more recently in ferrets (3, 24, 35). In mice, it was shown that influenza viruses could enter the CNS via the olfactory nerve and trigeminal nerve from the nasal cavity (27, 28, 31, 32, 39) but also via the vagal nerves and sympathetic nerves from the lungs (31). In ferrets, HPAI H5N1 virus

Received 16 November 2011 **Accepted** 6 January 2012
Published ahead of print 25 January 2012
Address correspondence to Debby van Riel, d.vanriel@erasmusmc.nl.

doi:10.1128/JVI.06828-11

most likely entered the CNS via the olfactory nerve (3, 35). However, virus entry via the olfactory nerve, through infection of olfactory receptor neurons (ORNs), the axons of which extend directly into the olfactory bulb, has never been proven in ferrets. In mice, replication of neurotropic influenza viruses in ORNs has been described (1, 28).

Here we studied the systemic spread of HPAI H5N1 virus in ferrets, with a special focus on the olfactory route. Additionally, we determined the role of the MBCS of HPAI H5N1 virus in this systemic spread. To this end, ferrets were inoculated with HPAI H5N1 virus either with or without the MBCS, and virus replication and associated lesions were determined in multiple tissues at different time points.

MATERIALS AND METHODS

Cells and viruses. Madin-Darby canine kidney (MDCK) cells were cultured in Eagle minimal essential medium (EMEM; Lonza, Breda, The Netherlands) supplemented with 10% fetal calf serum (FCS), 100 IU/ml penicillin, 100 μg/ml streptomycin, 2 mM glutamine, 1.5 mg/ml sodium bicarbonate, 10 mM HEPES, and nonessential amino acids. 293T cells were cultured in Dulbecco modified Eagle medium (Lonza) supplemented with 10% FCS, 100 IU/ml penicillin, 100 μg/ml streptomycin, 2 mM glutamine, 1 mM sodium pyruvate, and nonessential amino acids.

Highly pathogenic avian influenza virus A/Indonesia/5/05 (H5N1) was isolated from a human case and passaged once in embryonated chicken eggs and once in MDCK cells. All eight gene segments were amplified by reverse transcription-PCR (RT-PCR), cloned in a modified version of the bidirectional reverse genetics plasmid pHW2000 (9, 13), and subsequently used to generate recombinant wild-type (WT) virus ($H5N1_{WT}$) by reverse genetics, as described elsewhere (9). For the generation of H5N1 virus without an MBCS ($H5N1_{\Delta MBCS}$), the cleavage site PQRERRRKKR ↓ G in the H5 HA plasmid was changed to PQIETR ↓ G by RT-PCR with specific primers. Primer sequences are available upon request.

Replication kinetics. Multistep replication kinetics were determined by inoculating MDCK cells in the presence and absence of 20 μg/ml trypsin (Lonza) with a multiplicity of infection (MOI) of 0.01 50% tissue culture infective dose ($TCID_{50}$) per cell in 2-fold. Supernatants were sampled at 6, 12, 24, and 48 h after inoculation, and the virus titers in these supernatants were determined as described below.

Virus titrations. Virus titers in nasal and throat swab specimens, homogenized tissue samples from inoculated ferrets, or samples from inoculated MDCK cells were determined by endpoint titration in MDCK cells. MDCK cells were inoculated with 10-fold serial dilutions of each sample, washed 1 h after inoculation with phosphate-buffered saline (PBS), and cultured in 200 μl of infection medium, consisting of EMEM supplemented with 100 U/ml penicillin, 100 μg/ml streptomycin, 2 mM glutamine, 1.5 mg/ml sodium bicarbonate, 10 mM HEPES, nonessential amino acids, and 20 μg/ml trypsin (Cambrex). Three days after inoculation, supernatants of infected cell cultures were tested for agglutinating activity using turkey erythrocytes as an indicator of virus replication in the cells. Infectious virus titers were calculated from four replicates by the method of Karber (17).

Western blotting. 293T cells were transfected with the plasmids expressing $H5N1_{WT}$ or $H5N1_{\Delta MBCS}$ HA gene segments using the $CaPO_4$ method. Cells were harvested 48 h after transfection and were treated either with PBS or with 2.5 μg/ml trypsin (Lonza) for 1 h at 37°C. Cells were lysed in hot lysis buffer and treated with 3× dissociation loading buffer for 5 min at 96°C as previously described (30). Cell lysates were subjected to electrophoresis in 10% SDS-polyacrylamide gels and blotted, and Western blots were incubated with 1:2,000 rabbit serum with antibodies to A/Hong Kong/156/97 (H5) and a 1:3,000-diluted peroxidase-labeled swine antirabbit antibody. Blots were developed with enhanced chemiluminescence Western blotting detection reagents.

Ferret experiments. All animal studies were approved by an independent animal ethics committee. All experiments were performed under animal biosafety level 3+ conditions. The ferret model used to study the pathogenicity and virus distribution of $H5N1_{WT}$ and $H5N1_{\Delta MBCS}$ viruses was described previously (29). Groups of 12 influenza virus-seronegative and Aleutian disease-negative female ferrets (*Mustela putorius furo*) were inoculated intranasally with 10^6 $TCID_{50}$ of $H5N1_{WT}$ or $H5N1_{\Delta MBCS}$ virus, divided over both nostrils (250 μl to each nostril). Throat and nose swab specimens were collected daily to determine virus excretion from the upper respiratory tract. Nose swab specimens were collected from only one nostril to keep the respiratory epithelium of the other nostril intact for pathology. Animals were weighed daily and observed for clinical signs as an indicator of disease. Three animals from each group were euthanized at 1, 3, 5, and 7 days postinoculation (dpi), and necropsies were performed according to a standard protocol. The trachea was clamped off so the lungs would not deflate upon opening of the pleural cavity, which allowed visual estimation of the area of lung parenchyma affected. Nasal turbinates (NT) containing both respiratory and olfactory mucosa, trachea, lungs, liver, spleen, kidney, colon, cervical spinal cord, pancreas, heart, cerebellum, cerebrum, serum, and cerebrospinal fluid (CSF) were collected to study virus distribution by virus titration. Half the head was fixed in 10% formalin, and multiple parts of the respiratory and olfactory epithelia from the nasal cavity and the olfactory bulb, cerebrum, cerebellum, and trigeminal nerve were collected for pathological investigation. Other tissues collected for pathological investigation were cervical spinal cord, tonsil, trachea, left lung, heart, liver, spleen, pancreas, duodenum, jejunum, colon, kidney, and adrenal gland.

Pathology and immunohistochemistry. During necropsy, samples for pathological examination were collected in 10% neutral-buffered formalin (samples were collected from lungs after inflation with formalin) and fixed for 7 days. Tissues were embedded in paraffin, sectioned at 3 μm, and stained with hematoxylin and eosin (HE) for the detection of histological lesions by light microscopy. For the detection of virus antigen by immunohistochemistry, tissues were stained with a monoclonal antibody against influenza A virus nucleoprotein as described previously (42).

Virus histochemistry. The attachment pattern of $H5N1_{WT}$ virus in olfactory epithelium and respiratory epithelium from control ferrets ($n = 2$) was determined as described previously (41). Briefly, reassortant virus consisting of six gene segments of influenza virus A/PR8/8/34 and the HA and PB2 segments of A/Indonesia/5/05 virus was propagated in MDCK cells and concentrated and purified using sucrose gradients. Concentrated virus was inactivated by dialysis against 0.1% formalin and labeled with fluorescein isothiocyanate (FITC). Paraffin-embedded tissues were incubated with FITC-labeled $H5N1_{WT}$ virus and detected with a peroxidase-labeled rabbit anti-FITC antibody (Dako, Heverlee, Belgium), and the signal was amplified with a tyramide signal amplification system (Perkin Elmer, Groningen, The Netherlands). Peroxidase was revealed with 3-amino-9-ethyl-carbazole, resulting in a red precipitate.

RESULTS

$H5N1_{\Delta MBCS}$ trypsin dependence *in vitro*. The functionality of the HA protein after deletion of the MBCS was investigated by expression of the HA of $H5N1_{WT}$ and $H5N1_{\Delta MBCS}$ viruses in 293T cells. The cleavage pattern was determined in the presence and absence of trypsin. Upon deletion of the MBCS, efficient cleavage of HA0 into HA1 and HA2 was observed only in the presence of trypsin, whereas the $H5N1_{WT}$ HA was cleaved in the absence of trypsin (Fig. 1A). Next, the effect of the deletion of the MBCS on the replication kinetics was determined in the absence and presence of trypsin (20 μg/ml). Via reverse genetics, $H5N1_{WT}$ and $H5N1_{\Delta MBCS}$ viruses were rescued. $H5N1_{WT}$ replicated to similar virus titers in the presence and absence of trypsin. In contrast, $H5N1_{\Delta MBCS}$ virus did not replicate efficiently in the absence of trypsin, which is in agreement with an LPAI virus phenotype (Fig.

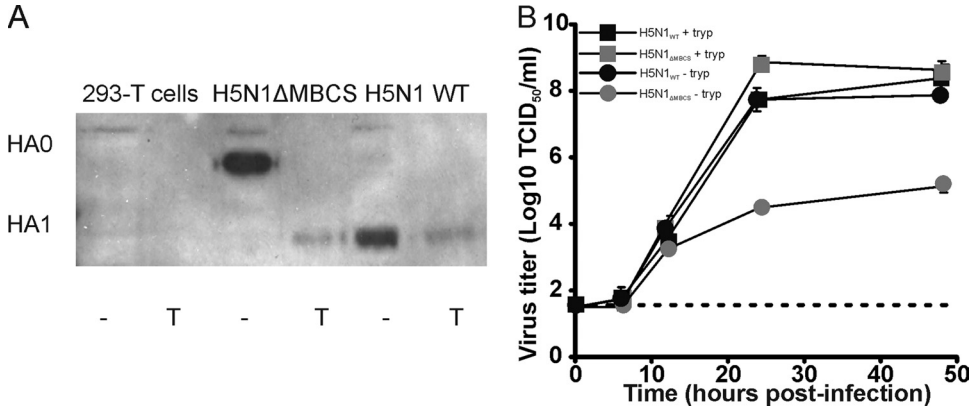

FIG 1 *In vitro* phenotype of $H5N1_{WT}$ and $H5N1_{\Delta MBCS}$ viruses. (A) Western blots of lysates of 293T cells untransfected or transfected with HAs of $H5N1_{\Delta MBCS}$ virus and $H5N1_{WT}$ virus upon treatment with (lanes T) or without (lanes −) trypsin. (B) Replication of $H5N1_{WT}$ virus and $H5N1_{\Delta MBCS}$ virus in MDCK cells in the presence or absence of trypsin (tryp). Geometric mean titers were calculated from two independent experiments; error bars indicate standard deviations. The lower limit of detection is indicated by the dotted line.

1B). $H5N1_{\Delta MBCS}$ virus is able to replicate for one round of infection. Thereafter, the HA of progeny released from $H5N1_{\Delta MBCS}$ cannot be cleaved, and therefore, the virus is no longer infectious.

Clinical signs and gross lesions in ferrets inoculated with $H5N1_{\Delta MBCS}$ virus were less severe than those in $H5N1_{WT}$ virus-inoculated ferrets. To determine the pathogenicity of HPAI H5N1 virus in ferrets, including systemic spread, and to elucidate the role of the MBCS, 12 ferrets were inoculated intranasally with 10^6 $TCID_{50}$ of $H5N1_{WT}$ or $H5N1_{\Delta MBCS}$ virus. Ferrets inoculated with $H5N1_{WT}$ virus developed anorexia and lethargy. In contrast, ferrets inoculated with $H5N1_{\Delta MBCS}$ virus did not reveal any clinical signs. Ferrets were weighed daily as an indicator of disease. The maximum weight loss was 20% (20% ± 1.6%) for animals inoculated with $H5N1_{WT}$ virus and occurred at 7 dpi, the end of the experiment. Ferrets inoculated with $H5N1_{\Delta MBCS}$ virus lost a maximum of 6% (6.0% ± 4.0%) of their body weight at 3 dpi, and their body weight returned to 100% at 7 dpi (Fig. 2A).

Gross pathological examination in ferrets inoculated with $H5N1_{WT}$ virus revealed multifocal dark red areas of consolidation in the lungs in 1/3, 2/3, 3/3, and 3/3 ferrets at 1, 3, 5, and 7 dpi, respectively, with a maximum of affected lung tissue of 37% (37% ± 39%) at 7 dpi. In ferrets inoculated with $H5N1_{\Delta MBCS}$ virus, 2/3 at 1, 3, and 7 dpi and 1/3 at 5 dpi showed multifocal dark red areas of consolidation in the lungs, with a maximum of affected lung tissue of 7% (7% ± 6%) at 7 dpi (Table 1). The relative lung weight had a maximum at 5 dpi for ferrets inoculated with $H5N1_{WT}$ and $H5N1_{\Delta MBCS}$ virus of 1.3% (1.3% ± 0.4%) and 1.0% (1.0% ± 0.4%), respectively (Table 1). Stomachs were empty in all ferrets inoculated with $H5N1_{WT}$ virus, with the exception of two ferrets at 1 dpi. Only two ferrets inoculated with $H5N1_{\Delta MBCS}$ virus revealed empty stomachs at 1 and 3 dpi (Table 1). These results indicate that the $H5N1_{\Delta MBCS}$ virus induced less severe disease than the $H5N1_{WT}$ virus when the body weight, clinical signs, and gross lesions are considered.

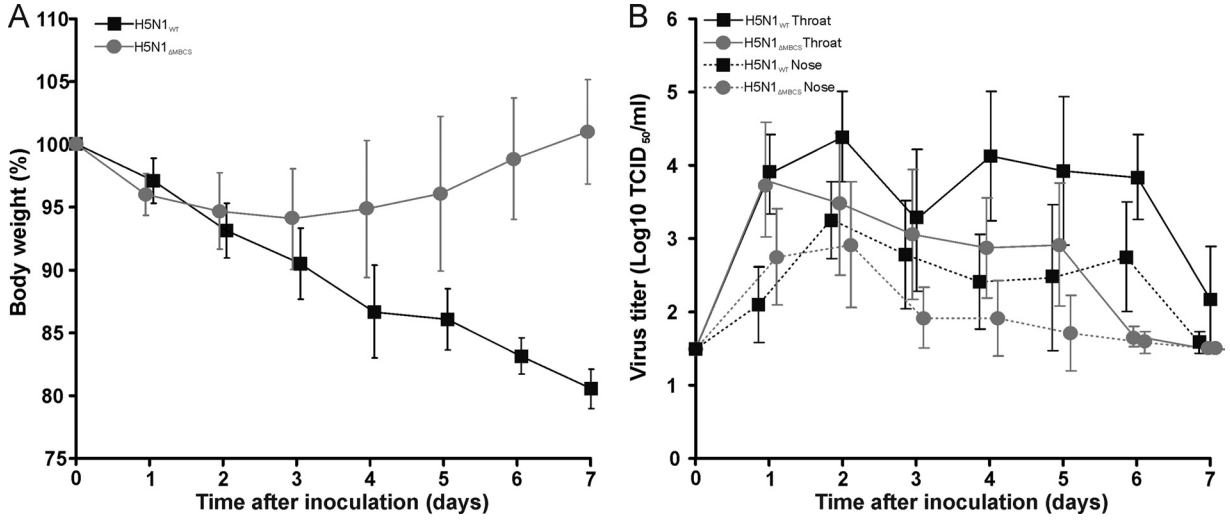

FIG 2 Weight loss and virus shedding in ferrets inoculated with $H5N1_{WT}$ or $H5N1_{\Delta MBCS}$ viruses. (A) Mean body weights and standard deviations are depicted as percentage of body weight at time of inoculation for each group inoculated with $H5N1_{WT}$ virus and $H5N1_{\Delta MBCS}$ virus. (B) Virus shedding from the upper respiratory tract of ferrets inoculated with $H5N1_{WT}$ virus or $H5N1_{\Delta MBCS}$ virus from the nose and throat is indicated. Geometric mean titers are shown, with error bars provided to indicate the standard deviations. The lower limit of detection is 1.5 $\log_{10}$ $TCID_{50}$.

TABLE 1 Gross pathology in ferrets inoculated with $H5N1_{WT}$ virus or $H5N1_{\Delta MBCS}$ virus

Virus	dpi	Animals with macroscopic lung lesions[a]	Area of lung affected (%)[b]	Relative lung wt (%)	Empty stomach[c]
$H5N1_{WT}$	1	1/3	2 ± 3	0.7 ± 0.0	1/3
	3	2/3	3 ± 3	0.7 ± 0.0	3/3
	5	3/3	29 ± 23	1.3 ± 0.4	3/3
	7	3/3	37 ± 39	1.3 ± 0.7	3/3
$H5N1_{\Delta MBCS}$	1	2/3	3 ± 3	0.8 ± 0.1	1/3
	3	2/3	5 ± 5	0.8 ± 0.2	1/3
	5	1/3	2 ± 3	1.0 ± 0.4	0/3
	7	2/3	7 ± 6	0.8 ± 0.1	0/3

[a] Number of ferrets in which macroscopic lung lesions were detected/total number of ferrets are depicted.
[b] Area of lung affected and relative lung weight are reported as means ± standard deviations ($n = 3$).
[c] Number of ferrets with empty stomachs/total number of ferrets are depicted.

Virus isolation from swabs and organs differs between $H5N1_{WT}$ and $H5N1_{\Delta MBCS}$ virus-inoculated ferrets. Nose and throat swab specimens were collected daily, and virus titers were determined by endpoint titration in MDCK cells. Nose swabs remained positive up to 7 dpi in $H5N1_{WT}$ virus-inoculated ferrets and up to 6 dpi in $H5N1_{\Delta MBCS}$ virus-inoculated ferrets (Fig. 2B). Virus shedding from the throat continued up to 7 and 6 dpi for $H5N1_{WT}$ and $H5N1_{\Delta MBCS}$ virus-inoculated ferrets, respectively (Fig. 2B). Shedding from the respiratory tract of $H5N1_{\Delta MBCS}$ virus-inoculated ferrets appears to be lower than that from $H5N1_{WT}$ virus-inoculated ferrets, indicative of less efficient virus replication.

At 1, 3, 5, and 7 dpi, three ferrets from each group were euthanized and NT, trachea, lungs, liver, spleen, kidney, colon, spinal cord, pancreas, heart, cerebellum, cerebrum, serum, and CSF were collected and virus titers were determined. The virus titers in samples from lung and trachea were similar at 1, 3, and 5 dpi between $H5N1_{WT}$ virus- and $H5N1_{\Delta MBCS}$ virus-inoculated ferrets. However, in NT the virus titers were 3.0 $\log_{10}$ $TCID_{50}$ lower in $H5N1_{\Delta MBCS}$ virus-inoculated ferrets than in $H5N1_{WT}$ virus-inoculated ferrets at 1, 3, and 5 dpi. At 7 dpi, virus was undetectable in all samples from $H5N1_{\Delta MBCS}$ virus-inoculated ferrets, indicating that the animals cleared the virus by this time point (Table 2).

Infectious virus was isolated from extrarespiratory tissues of $H5N1_{WT}$ virus-inoculated ferrets from 3 dpi onwards. At 3 dpi, infectious virus was found in one colon sample. At 5 dpi, infectious virus was found in the liver (3/3), pancreas (1/3), and heart (2/3). At 7 dpi, extrarespiratory infectious virus was detected in the liver (3/3), pancreas (2/3), colon (2/3), heart (1/3), spinal cord (1/3), cerebellum (2/3), and cerebrum (3/3). In contrast, $H5N1_{\Delta MBCS}$ virus-inoculated ferrets did not reveal any extrarespiratory infectious virus. Infectious virus was not detected in spleen or kidney at any of the time points in $H5N1_{WT}$ virus-inoculated ferrets. Interestingly, at 7 dpi we detected infectious virus in the CSF. No infectious virus could be isolated from the serum of $H5N1_{WT}$ virus-inoculated ferrets (Table 2). Nevertheless, low levels of viral genomic RNA were detected in serum by quantitative RT-PCR from 1/3, 2/3, 1/3, and 3/3 ferrets at 1, 3, 5, and 7 dpi, respectively (data not shown). No infectious virus was isolated from extrarespiratory tissues, serum, or CSF of $H5N1_{\Delta MBCS}$ virus-inoculated ferrets.

Distribution of virus antigen is more widespread in $H5N1_{WT}$ virus-inoculated ferrets than $H5N1_{\Delta MBCS}$ virus-inoculated ferrets. The distribution of virus antigen in cerebrum, cerebellum, trigeminal nerve, NT, spinal cord, tonsil, trachea, left lung, heart, liver, spleen, pancreas, duodenum, jejunum, colon, kidney, and

TABLE 2 Virus titers in tissues and CSF of ferrets inoculated with $H5N1_{WT}$ virus or $H5N1_{\Delta MBCS}$ virus

	Virus titer ($\log_{10}$ $TCID_{50}$/g tissue)							
	$H5N1_{WT}$				$H5N1_{\Delta MBCS}$			
Tissue	Day 1	Day 3	Day 5	Day 7	Day 1	Day 3	Day 5	Day 7
Respiratory system								
Nasal turbinates	6.0 ± 0.7 (3/3)[a]	7.2 ± 0.9 (3/3)	6.6 ± 0.8 (3/3)	6.2 ± 0.2 (3/3)	3.0 ± 0.0 (2/3)	4.2 ± 0.6 (2/3)	3.6 ± 0.3 (3/3)	<1.2[b]
Trachea	2.9 ± 0.7 (3/3)	3.2 (1/2)[c]	3.4 ± 0.2 (2/3)	3.9 ± 0.6 (2/3)	3.0 ± 0.3 (3/3)	1.9 (1/3)	3.9 ± 2.8 (3/3)	<1.7
Lung	2.0 ± 0.7 (2/3)	2.9 (1/3)	5.3 ± 1.7 (3/3)	4.2 ± 2.3 (2/3)	2.9 ± 0.2 (3/3)	1.8 (1/3)	3.9 ± 2.2 (2/3)	<1.3
Nervous system								
Cerebrum	<1.5	<1.5	<1.5	2.1 ± 0.2 (3/3)	<1.5	<1.5	<1.5	<1.5
Cerebellum	<1.7	<1.7	<1.7	3.7 ± 0.0 (2/3)	<1.7	<1.7	<1.7	<1.7
Spinal cord	<1.7	<1.7	<1.7	2.1 (1/3)	<1.7	<1.7	<1.7	<1.7
Cerebrospinal fluid[d]	<1.5	<1.5	<1.5	3.8 ± 0.7 (2/3)	<1.5	<1.5	<1.5	<1.5
Other								
Pancreas	<1.5	<1.5	3.0 (1/3)	2.9 ± 0.5 (2/3)	<1.5	<1.5	<1.5	<1.5
Liver	<1.1	<1.1	2.8 ± 0.9 (3/3)	4.4 ± 1.1 (3/3)	<1.1	<1.1	<1.1	<1.1
Colon	<1.4	2.1 (1/3)	<1.4	1.8 ± 0.1 (2/3)	<1.4	<1.4	<1.4	<1.4
Heart	<1.5	<1.5	2.1 ± 0.3 (2/3)	2.3 (1/3)	<1.5	<1.5	<1.5	<1.5

[a] Virus titers are reported as means ± standard deviations ($n = 3$) or as individual titers if viruses were not isolated from all three animals. Number of ferrets in which virus positive organs were detected/total number of ferrets are depicted.
[b] Cutoff values are given for negative tissues.
[c] Only two tracheal tissue samples were collected.
[d] Virus titers of cerebrospinal fluid are in $\log_{10}$ $TCID_{50}$/ml.

TABLE 3 Detection of influenza A virus nucleoprotein in tissues from ferrets inoculated with either $H5N1_{WT}$ virus or $H5N1_{\Delta MBCS}$ virus

Tissue	$H5N1_{WT}$				$H5N1_{\Delta MBCS}$			
	Day 1	Day 3	Day 5	Day 7	Day 1	Day 3	Day 5	Day 7
Respiratory system								
Respiratory epithelium	+/− (3/3)[a]	+/− (3/3)[b]	+/− (3/3)[b]	−[c]	+/− (2/3)	+/− (1/3)[b]	−	−
Olfactory epithelium	+/− (3/3)	+ (3/3)[b,d]	+ (3/3)[b]	+ (3/3)[b]	+/− (2/3)	+ (3/3)[b]	+/− (2/3)[b]	+ (2/3)
Trachea	−	−	−	+/− (1/3)	−	−	+/− (2/3)[b]	−
Bronchus	−	−	−	+/− (1/3)[b]	−	−	−	−
Bronchioles	−	−	+ (1/3)[b]	+ (1/3)[b]	−	−	+/− (1/3)[b]	−
Alveoli	−	+ (1/3)[b]	+ (3/3)[b]	−	−	+ (1/3)[b]	+ (1/3)[b]	−
Nervous system								
Olfactory bulb	−	+ (1/3)[b]	+ (2/3)[b]	+ (3/3)[b]	−	−	−	−
Cerebrum	−	−	+ (1/3)[b]	+ (2/3)[b]	−	−	−	−
Cerebellum	−	−	−	+ (1/3)[b]	−	−	−	−
Spinal cord	−	−	−	+ (1/3)[b]	−	−	−	−
Trigeminal nerve	−	−	+ (1/3)[b]	−	−	−	−	−
Other								
Pancreas	−	−	−	+ (1/3)[b]	−	−	−	−
Liver	−	−	−	+ (2/3)[b]	−	−	−	−
Tonsils	−	+ (1/1)[b,e]	+ (1/3)[b]	−	−	−	−	−

[a] +/−, <10 cells contained virus antigen.
[b] The detection of virus antigen was associated with histological lesions.
[c] −, virus antigen was not detected.
[d] +, >10 cells contained virus antigen.
[e] Only one tonsil was sampled.

adrenal gland from ferrets inoculated with $H5N1_{WT}$ or $H5N1_{\Delta MBCS}$ virus was determined on 1, 3, 5, and 7 dpi (Table 3). In ferrets inoculated with $H5N1_{WT}$ virus, virus antigen was detected in the respiratory tract from 1 dpi onward. In the NT, virus antigen was observed in only a few respiratory epithelial cells at 1, 3, and 5 dpi. Virus antigen was present in a few olfactory receptor neurons at 1 dpi but was abundantly present at 3, 5, and 7 dpi, with a peak at 3 dpi (Fig. 3). Interestingly, virus antigen was also observed in the Bowman's glands and the olfactory ensheathing cells in the lamina propria of the olfactory mucosa (Fig. 4). In the lower respiratory tract, virus antigen was present in 1/3 ferrets at 3 dpi, 3/3 at 5 dpi, and 1/3 at 7 dpi. Virus antigen was most commonly found in alveolar epithelial cells and in 2/3 ferrets (5 and 7 dpi) in epithelial cells of the bronchioles, bronchus, and trachea (Table 3).

In the nervous system of $H5N1_{WT}$ virus-inoculated animals, virus antigen was found in 0/3, 1/3, 3/3, and 3/3 ferrets at 1, 3, 5, and 7 dpi, respectively (Tables 3 and 4). At 3 dpi, virus antigen was first observed in periglomerular cells in the glomerular layer of the olfactory bulb, where the axons of the olfactory receptor neurons have contact with both second-order neurons and periglomerular cells in the olfactory bulb. At 5 dpi, virus antigen was observed in the periglomerular cells of the olfactory bulb, in glial cells in the cerebrum, and in one neuron in the trigeminal nerve. At 7 dpi, virus antigen was found in mitral cells and granular cells in the olfactory bulb, in glial cells and neuronal cells in the olfactory tract, in glial cell and neuronal cells in the cerebrum and cerebellum, in meningeal cells surrounding the cerebrum, cerebellum, and spinal cord, and in ependymal cells in the choroid plexus around the cerebellum (Fig. 4).

Beyond the respiratory tract and CNS, virus antigen was observed in lymphoid cells in the tonsils at 3 and 5 dpi, in hepatocytes in the liver at 7 dpi, and in acinar cells in the pancreas at 7 dpi (Table 3; Fig. 5). No virus antigen was detected in tissues of the heart, adrenal gland, kidney, spleen, duodenum, jejunum, or colon.

In ferrets inoculated with $H5N1_{\Delta MBCS}$ virus, virus antigen expression was restricted to the respiratory tract (Table 3). Virus antigen was found in only a few respiratory epithelial cells at 1 and 3 dpi. In the olfactory epithelium, virus antigen was observed in 2/3, 3/3, 2/3, and 2/3 ferrets at 1, 3, 5, and 7 dpi, respectively (Fig. 3). Overall, the number of olfactory receptor neurons that contained virus antigen was lower in the $H5N1_{\Delta MBCS}$ virus-inoculated ferrets than in the $H5N1_{WT}$ virus-inoculated ferrets. There was no evidence of virus antigen in the Bowman's glands or olfactory ensheathing cells in the $H5N1_{\Delta MBCS}$ virus-inoculated ferrets.

Histological lesions in ferrets inoculated with $H5N1_{WT}$ virus were more severe than those in $H5N1_{\Delta MBCS}$ virus-inoculated ferrets. Association of histological lesions and influenza virus infection was based on colocalization of lesions and influenza virus antigen. Influenza virus-associated lesions in $H5N1_{WT}$ virus-inoculated ferrets predominated in the nasal cavity, central nervous system, and lower respiratory tract and were less frequent in liver, pancreas, and tonsils (Table 3). Influenza virus-associated lesions in $H5N1_{\Delta MBCS}$ virus-inoculated ferrets were restricted to the nasal cavity and lower respiratory tract.

Lesions in both the olfactory and respiratory epithelia of the nasal cavity occurred commonly in $H5N1_{WT}$ virus-inoculated ferrets (Table 3), but the lesions were much more extensive and severe in the olfactory mucosa than in the respiratory mucosa. Olfactory mucosa lesions consisted of a moderate or severe, multifocal necrotizing rhinitis, characterized at 3 dpi by necrosis of olfactory epithelial cells and of epithelial cells of the underlying Bowman's glands and infiltration by moderate numbers of partly

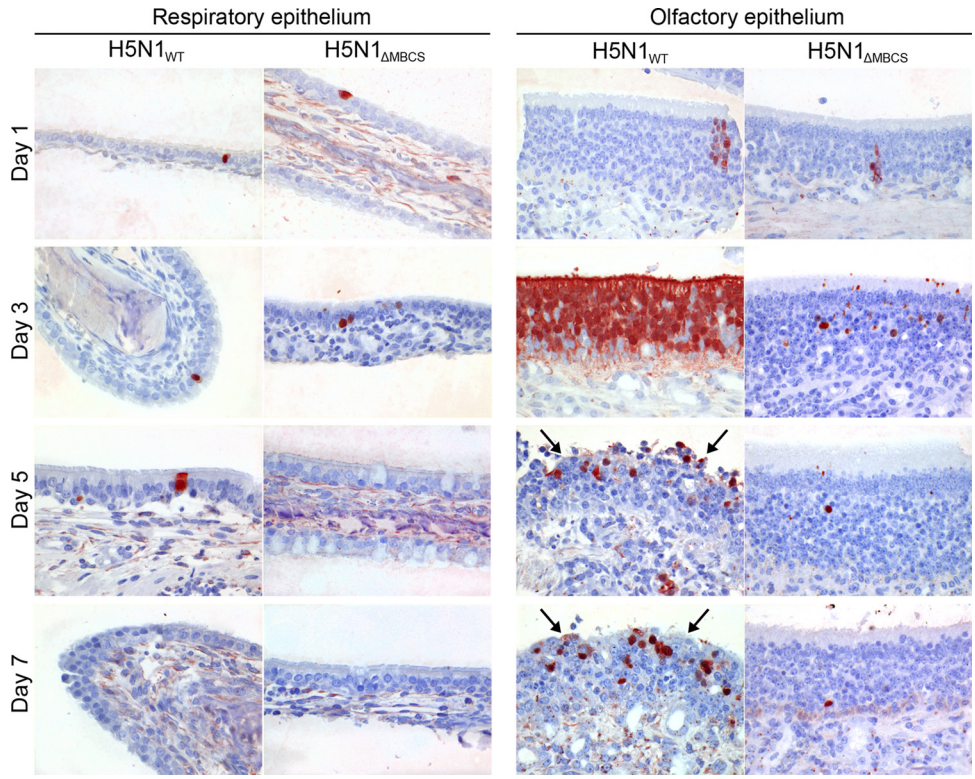

FIG 3 Influenza virus antigen expression in respiratory epithelium and olfactory epithelium of ferrets inoculated with either $H5N1_{WT}$ virus or $H5N1_{\Delta MBCS}$ virus. Influenza virus antigen in the respiratory epithelium and olfactory epithelium in ferrets inoculated with $H5N1_{WT}$ or $H5N1_{\Delta MBCS}$ virus at 1, 3, 5, and 7 dpi. Tissue sections were stained with a monoclonal antibody against influenza A virus nucleoprotein, visible as red staining. In the respiratory epithelium, individual virus antigen-positive epithelial cells are observed at 1, 3, and 5 dpi in $H5N1_{WT}$ virus-inoculated ferrets and at 1 and 3 dpi in $H5N1_{\Delta MBCS}$ virus-inoculated ferrets. In the olfactory epithelium, virus antigen in $H5N1_{WT}$ virus-inoculated ferrets was present from 1 to 7 dpi, with a peak at 3 dpi. At days 5 and 7 dpi, there was focal severe necrosis of olfactory epithelial cells with infiltration of neutrophils (arrows). In the $H5N1_{\Delta MBCS}$ virus-inoculated ferrets, virus antigen was present from day 1 to 7. Magnification, ×400.

degenerated neutrophils. At 5 dpi, lesions progressed to multiple erosions of the olfactory mucosa adjacent to reactive hypertrophy and hyperplasia of remaining olfactory epithelial cells and disruption of the histological architecture of the Bowman's glands. The lesions at 7 dpi were similar to those at 5 dpi, but with the addition of hypertrophy and hyperplasia of remaining epithelial cells in the Bowman's glands. In comparison, respiratory mucosa lesions consisted of a mild, focal rhinitis, characterized by infiltration of a few neutrophils in the respiratory epithelium and underlying connective tissue. Lesions in the olfactory and respiratory epithelia were less common in $H5N1_{\Delta MBCS}$ virus-inoculated ferrets (Table 3) and milder in character.

Lesions in the central nervous system of $H5N1_{WT}$ virus-inoculated ferrets first occurred in the olfactory bulb of single ferrets at 3 and 5 dpi and were subsequently widespread throughout the central nervous system of all ferrets at 7 dpi (Table 4; Fig. 4). Olfactory bulb lesions consisted of a focal infiltration with rare neutrophils in the glomerular layer at 3 dpi. At 5 dpi, olfactory bulb lesions had extended to multifocal infiltration with moderate numbers of neutrophils in the glomerular and granular layers, as well as perivascular cuffing with mononuclear cells and neutrophils. At 7 dpi, lesions were similar to those at 5 dpi, except that they were restricted to the granular layer and perivascular cuffing consisted predominantly of mononuclear cells. At 7 dpi, lesions were also present in the olfactory tract, cerebrum, cerebellum, and spinal cord. In general, these lesions consisted of multiple foci of neuronal necrosis, infiltration by moderate numbers of partly degenerate neutrophils, and perivascular cuffing with mononuclear cells. The leptomeninges overlying these tissues were infiltrated by many mononuclear cells and occasional neutrophils. In addition to cerebellar lesions, two ferrets also had necrosis and sloughing of adjacent ependymal cells and edema of the underlying neuropil.

Lesions in the lower respiratory tract were present in five $H5N1_{WT}$ virus-inoculated ferrets (Table 3) and were mild and focal except in one ferret at 5 dpi, in which they were moderate and locally extensive. In general, lesions were centered on alveoli and bronchioles, with milder and less frequent lesions occurring in bronchi and trachea. At 3 dpi, the lesions were characterized by necrosis and loss of alveolar and bronchiolar epithelial cells, infiltration of neutrophils in alveolar and bronchiolar walls, and the presence of neutrophils mixed with fibrin in alveolar and bronchiolar lumina. At 5 and 7 dpi, mononuclear cells progressively predominated over neutrophils in the inflammatory cell infiltrate, and there was hypertrophy and hyperplasia of epithelial cells in both alveoli and bronchioles. Lesions in the lower respiratory tract of ferrets inoculated with $H5N1_{\Delta MBCS}$ virus were present in single ferrets at 3, 5, and 7 dpi. These lesions were focal and comparable in appearance to those in ferrets inoculated with $H5N1_{WT}$ virus.

Lesions outside the nervous and respiratory systems were restricted to the liver, pancreas, and tonsils of ferrets inoculated with

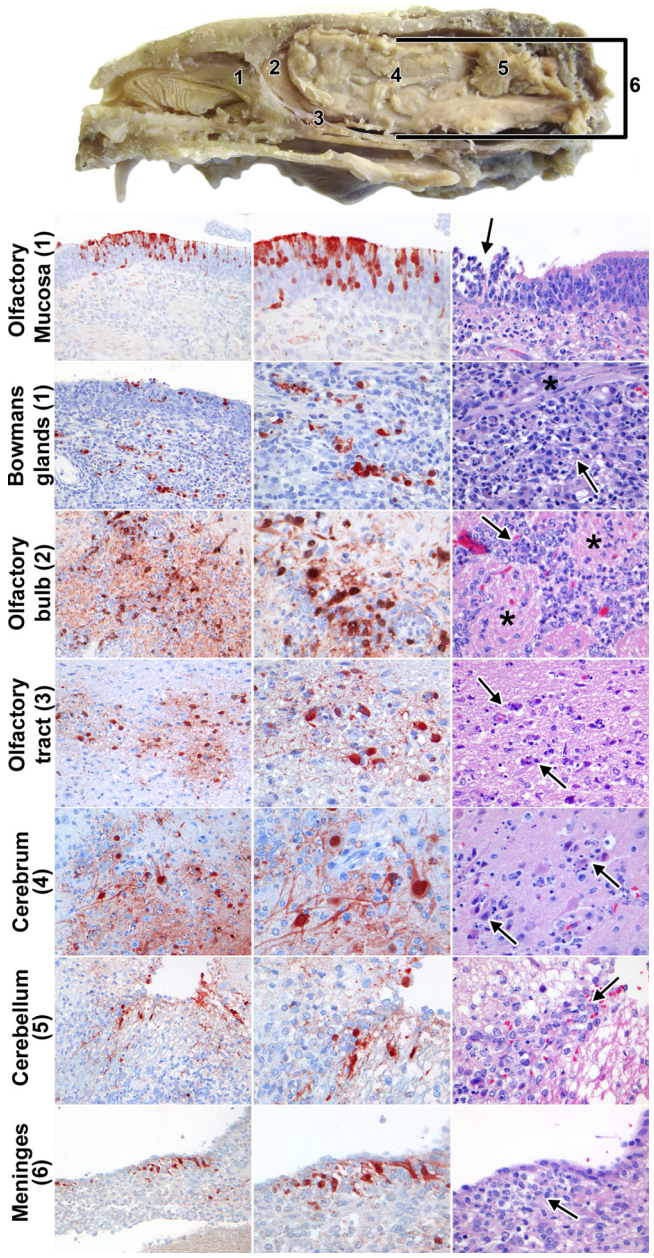

FIG 4 Detection of histological lesions or influenza A virus antigen expression in tissues from the nervous system of ferrets inoculated with $H5N1_{WT}$ virus. A cross section of a ferret head to illustrate the different anatomical sites is shown at the top. The nasal cavity contains the nasal turbinates, which are lined by respiratory mucosa, except at the back and top of the cavity, where they are lined by olfactory mucosa (position 1). The olfactory bulb (position 2) is separated from the nasal cavity by the cribriform plate and connected via the olfactory tract (position 3) to the cerebrum (position 4). The cerebellum (position 5), cerebrum, olfactory bulb, and olfactory tract are all surrounded by the meninges (position 6). (Left and middle columns) Immunohistochemistry for influenza A virus antigen in different tissues of the olfactory route. Magnifications, ×200 and ×400, left and middle columns, respectively. (Right column) Histological lesions in different tissues of the olfactory route. Magnification, ×400. Olfactory epithelium (position 1), which contained virus antigen from 1 dpi in olfactory receptor neurons, with focal necrosis of olfactory epithelial cells associated with infiltrating neutrophils (arrow); Bowman's glands (position 1), which contained virus antigen from 3 dpi, with necrosis of Bowman's gland epithelial cells associated with infiltrating neutrophils (arrow) along the nerve twigs (*); olfactory bulb (position 2), which contained virus antigen from 3 dpi, with infiltrating neutrophils (arrow) between the glomeruli (*) in the glomerular layer; olfactory tract (position 3), which contained virus antigen from 7 dpi, with neuronal necrosis and infiltrating neutrophils (arrows); cerebrum (position 4), which contained virus antigen from 5 dpi, with neuronal necrosis and infiltrating neutrophils (arrows); cerebellum (position 5), which contained virus antigen from 7 dpi, with neuronal necrosis and infiltrating neutrophils (arrow); meninges (position 6), which contained virus antigen from 7 dpi, with infiltration of many mononuclear cells and occasional neutrophils (arrow).

TABLE 4 Presence of histological lesions and presence of virus antigen in tissues that belong to the nervous system in ferrets inoculated with HPAI $H5N1_{WT}$ virus

Nervous system tissue	No. of ferrets with histological lesions/no. with virus antigen expression at each day			
	Day 1 ($n = 3$)	Day 3 ($n = 3$)	Day 5 ($n = 3$)	Day 7 ($n = 3$)
Olfactory epithelium	0/3	3/3	3/3	3/3
Olfactory bulb	0/0	0/1	1/2	3/3
Cerebrum	0/0	0/0	0/1	3/2
Cerebellum	0/0	0/0	0/0	2/1
Spinal cord	0/0	0/0	0/0	1/1
Leptomeninges	0/0	0/0	1/0	3/1
Choroid plexus	0/0	0/0	0/3	0/1

$H5N1_{WT}$ virus. In the liver, lesions were present in two ferrets at 7 dpi (Table 3; Fig. 5). These lesions consisted of multifocal necrosis of hepatocytes and replacement by variable proportions of neutrophils and mononuclear cells. Additionally, there was bile duct hyperplasia. In the pancreas of one ferret at 7 dpi, there was multifocal necrosis of pancreatic acinar cells, with widespread edema and infiltration of neutrophils and mononuclear cells. In the tonsils of single ferrets at 3 and 5 dpi, there was focal and mild (3 dpi) or multifocal and moderate (5 dpi) lymphocytic necrosis in the lymphoid tissue, with infiltration of neutrophils.

$H5N1_{WT}$ virus attaches abundantly to olfactory epithelium. To explain the differences in numbers of cells infected between the respiratory epithelium and olfactory epithelium in ferrets inoculated with $H5N1_{WT}$ virus, we determined the pattern of attachment of $H5N1_{WT}$ virus to these tissues from the nose of uninfected ferrets. There was no attachment of $H5N1_{WT}$ virus to respiratory epithelium, which is in accordance with previous observations (5). However, $H5N1_{WT}$ virus was able to attach abundantly to the apical side of the olfactory epithelium (Fig. 6). $H5N1_{\Delta MBCS}$ virus reveals the same attachment pattern, since the receptor preference of the virus has not been changed, as was shown by Chutinimitkul et al. (5).

DISCUSSION

This study improves our knowledge of systemic spread of HPAI H5N1 virus in a mammalian model in two respects. First, we show that the olfactory epithelium forms an island of susceptible cells in a sea of relatively resistant respiratory epithelium. From this island, HPAI H5N1 virus spreads directly to the CNS via the olfactory route. Second, we show that the MBCS is necessary for systemic spread of HPAI H5N1 virus. In its absence, the virus is restricted to the respiratory tract.

Intranasal inoculation of HPAI $H5N1_{WT}$ virus resulted in respiratory tract infection, characterized by extensive replication and lesions in the olfactory epithelium. The abundant attachment and replication of HPAI $H5N1_{WT}$ virus in cells of the olfactory

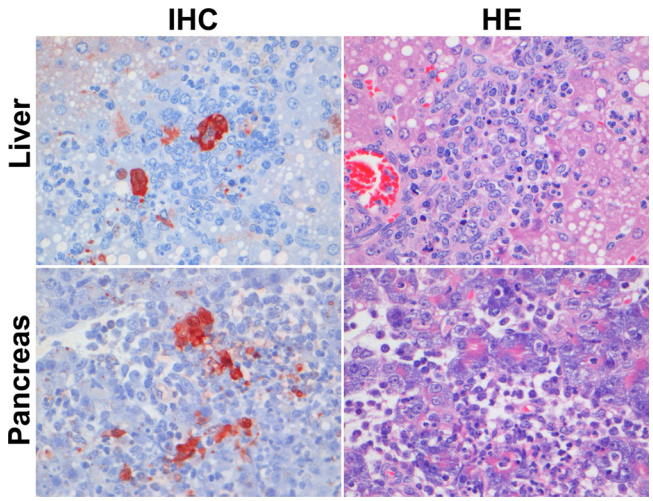

FIG 5 Detection of histological lesions (HE) and influenza A virus antigen (IHC) expression in extrarespiratory tract tissues in ferrets inoculated with $H5N1_{WT}$ virus. In the liver, virus antigen was observed in hepatocytes, with multifocal necrosis of hepatocytes and replacement by variable numbers of neutrophils and mononuclear cells. In the pancreas, virus antigen was observed in acinar cells, with necrosis of acinar cells, widespread edema, and infiltration of neutrophils and mononuclear cells. IHC, immunohistochemistry.

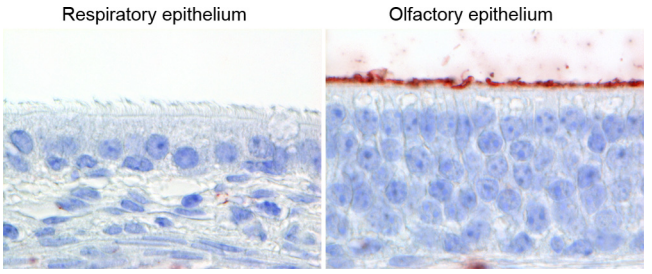

FIG 6 Attachment of $H5N1_{WT}$ virus to ferret respiratory epithelium and olfactory epithelium in the nose. No attachment of $H5N1_{WT}$ virus to the apical side of respiratory epithelium and abundant attachment of $H5N1_{WT}$ virus to the apical side of the olfactory epithelium. Tissue sections were incubated with $H5N1_{WT}$ virus; attachment is visible as red staining. Magnification, ×1,000.

epithelium explain the origin of the high virus titers found in homogenized NT. Virus antigen in the olfactory epithelium peaks at 3 dpi (Fig. 3), which corresponded with a peak in infectious virus titers in the NT at 3 dpi (Table 2) and nose swabs at 2 dpi (Fig. 2). The lack of abundant virus replication in the respiratory epithelium is consistent with the rare attachment of H5N1 virus (Fig. 6). Furthermore, low replication in the respiratory epithelium explains the relatively low virus titers found in the nasal swabs compared to the titers found after inoculation with a seasonal H3N2 virus (34). It is therefore tempting to speculate that a switch from replication in the olfactory epithelium to replication in the respiratory epithelium would result in higher virus titers in nasal swabs and possibly efficient respiratory droplet transmission (36a). Interestingly, intranasal inoculation of H5N1 virus did not result in a consistent severe inflammation of the lower respiratory tract, which is in accordance with the findings of a previous study by Bodewes et al. (3).

There was evidence for two routes of extrarespiratory spread in the HPAI $H5N1_{WT}$ virus-inoculated ferrets: first, via the olfactory route to the CNS and, second, via the hematogenous route. First, HPAI H5N1 virus is able to directly infect and replicate extensively in ORNs in the olfactory epithelium, from which it spread to the olfactory bulb and further into the CNS. The ORNs, which were influenza virus antigen positive from 1 dpi onwards, have axons that extend through the cribriform plate into the glomerular layer of the olfactory bulb. These axons synapse with periglomerular cells and neurons in the olfactory bulb, which contained virus antigen from 3 dpi onwards. Since it has been shown for HPAI viruses that transaxonal transport is possible (16, 26), infection of ORNs provides a direct route for H5N1 virus into the olfactory bulb. From 5 dpi onwards, virus spread along the olfactory tract into the cerebrum and cerebellum was observed. Infectious virus was detected at 7 dpi in CSF, together with virus antigen in the meninges, choroid plexus, and ependymal cells, providing an additional route of virus spread throughout the CNS from 7 dpi onwards, as described before (3). The observation that HPAI $H5N1_{WT}$ virus spreads to the CNS without severe respiratory disease fits with a case report of two children with acute encephalitis without initial respiratory disease. HPAI H5N1 virus was retrospectively detected in the CSF from one of these children (8). It remains to be determined if virus entry via the olfactory route is a unique feature of A/Indonesia/5/05 HPAI H5N1 virus or if other HPAI H5N1 strains and possibly seasonal influenza viruses are also able to enter the CNS via the olfactory route in the ferret model (24).

Besides the olfactory route, there was also evidence for HPAI $H5N1_{WT}$ virus spread via the hematogenous route. The pattern of virus distribution in colon, pancreas, heart, and liver is indicative of blood-borne spread, which correlates with the detection of viral genomic RNA in serum. Hematogenous spread into the CNS appears to be less likely, considering the observed virus distribution along the olfactory route. This is also in agreement with previous studies that also suggest that the olfactory tract is a route of entry into the CNS (3, 35).

The extrarespiratory spread observed in the HPAI $H5N1_{WT}$ virus-inoculated ferrets was dependent on the MBCS, since replication was restricted to the respiratory tract in $H5N1_{\Delta MBCS}$ virus-inoculated ferrets. In addition, clinical disease was also dependent on the MBCS since ferrets inoculated with $H5N1_{\Delta MBCS}$ virus revealed fewer symptoms than $H5N1_{WT}$ virus-inoculated ferrets. The role of the MBCS in H5N1 virus in the extrarespiratory spread in ferrets corresponds with observations in chickens and mice (12, 14). However, the mechanism by which HPAI H5N1 virus spreads beyond the respiratory tract varies largely between chickens and mammals. In chickens, the acquisition of an MBCS results in an endothelial cell tropism, which facilitates systemic replication in endothelial cells and subsequent replication in extrarespiratory organs (38). In contrast, in mammals—and some bird species—the presence of an MBCS in H5N1 virus results in systemic replication of H5N1 virus, without extensive replication in endothelial cells (18, 21). Interestingly, the presence of an MBCS in a seasonal H3N2 virus did not result in systemic dissemination (34). This lack of systemic dissemination might be due in part to a difference in cell tropism in the respiratory tract. Seasonal H3N2 virus and HPAI H5N1 virus recognize different sialic acids and are known to target different cell types in both the upper and lower respiratory tract (40, 41).

Replication of $H5N1_{\Delta MBCS}$ virus—which was trypsin dependent *in vitro*—was strongly reduced in the nose (Table 2) both in virus titers and in numbers of influenza virus-positive cells in the

olfactory mucosa compared to $H5N1_{WT}$ virus (Fig. 3). However, this difference was not observed as clearly in the virus titers from the nose swabs, probably due to the overall low viral shedding from the nose. However, virus replication in the lower respiratory tract was not reduced early after inoculation compared with that in $H5N1_{WT}$ virus-inoculated ferrets. Since the HA of $H5N1_{\Delta MBCS}$ virus cannot be cleaved by intracellular furin-like proteases, activation of the HA of this virus is dependent on cell membrane and soluble proteases. This could indicate that expression of these proteases varies between the different anatomical sites and cell types in the respiratory tract of ferrets. In rats, the composition of proteases and inhibitory compounds varies largely between different anatomical sites in the respiratory tract (19). In humans, mucus on top of the human olfactory epithelium contains protease inhibitors (6). Further studies into the protease and protease inhibitor composition and their role in cell tropism and pathogenicity of influenza viruses in mammals are therefore required. Ferrets inoculated with $H5N1_{\Delta MBCS}$ revealed no systemic replication. Lack of virus spread along the olfactory tract might be the result of low virus titers in the upper respiratory tract and/or the absence of the appropriate proteases outside the respiratory tract in ferrets. The low virus titers in the nose might not be sufficient for a spillover to the olfactory bulb and CNS. However, it is not known if the appropriate proteases are present along the olfactory route in ferrets. Studies in the rat CNS have shown that trypsin I, which was able to cleave the HA of multiple influenza viruses, is present but not equally distributed throughout cells of and locations in the CNS (19).

In conclusion, HPAI $H5N1_{WT}$ virus is able to directly infect and replicate extensively in olfactory receptor neurons in the olfactory epithelium, from which it spreads to the olfactory bulb and further to the CNS. Interestingly, this entrance via the olfactory route was dependent on the presence of the MBCS in influenza virus A/Indonesia/5/05. Future studies should reveal whether this CNS invasion is a unique feature of HPAI H5N1 virus or whether more influenza viruses are able to enter the CNS via the olfactory route.

ACKNOWLEDGMENTS

We thank D. de Meulder, G. van Amerongen, and F. van de Panne for excellent technical assistance.

This research was financed through NIAID-NIH contract HHSN266200700010C, the ERC (Fluplan 250136), the EU (Antigone, FP7 278976), and the VIRGO Consortium (BSIK03012).

REFERENCES

1. **Aronsson F, Robertson B, Ljunggren HG, Kristensson K.** 2003. Invasion and persistence of the neuroadapted influenza virus A/WSN/33 in the mouse olfactory system. Viral Immunol. **16**:415–423.
2. **Bertram S, Glowacka I, Steffen I, Kuhl A, Pohlmann S.** 2010. Novel insights into proteolytic cleavage of influenza virus hemagglutinin. Rev. Med. Virol. **20**:298–310.
3. **Bodewes R, et al.** 2011. Pathogenesis of influenza A/H5N1 virus infection in ferrets differs between intranasal and intratracheal routes of inoculation. Am. J. Pathol. **179**:30–36.
4. **Chen J, et al.** 1998. Structure of the hemagglutinin precursor cleavage site, a determinant of influenza pathogenicity and the origin of the labile conformation. Cell **95**:409–417.
5. **Chutinimitkul S, et al.** 2010. In vitro assessment of attachment pattern and replication efficiency of H5N1 influenza A viruses with altered receptor specificity. J. Virol. **84**:6825–6833.
6. **Debat H, et al.** 2007. Identification of human olfactory cleft mucus proteins using proteomic analysis. J. Proteome Res. **6**:1985–1996.
7. **de Jong JC, Claas EC, Osterhaus AD, Webster RG, Lim WL.** 1997. A pandemic warning? Nature **389**:554.
8. **de Jong MD, et al.** 2005. Fatal avian influenza A (H5N1) in a child presenting with diarrhea followed by coma. N. Engl. J. Med. **352**:686–691.
9. **de Wit E, et al.** 2004. Efficient generation and growth of influenza virus A/PR/8/34 from eight cDNA fragments. Virus Res. **103**:155–161.
10. **Fouchier RA, et al.** 2005. Characterization of a novel influenza A virus hemagglutinin subtype (H16) obtained from black-headed gulls. J. Virol. **79**:2814–2822.
11. **Govorkova EA, et al.** 2005. Lethality to ferrets of H5N1 influenza viruses isolated from humans and poultry in 2004. J. Virol. **79**:2191–2198.
12. **Hatta M, Gao P, Halfmann P, Kawaoka Y.** 2001. Molecular basis for high virulence of Hong Kong H5N1 influenza A viruses. Science **293**:1840–1842.
13. **Hoffmann E, Neumann G, Kawaoka Y, Hobom G, Webster RG.** 2000. A DNA transfection system for generation of influenza A virus from eight plasmids. Proc. Natl. Acad. Sci. U. S. A. **97**:6108–6113.
14. **Horimoto T, Kawaoka Y.** 1994. Reverse genetics provides direct evidence for a correlation of hemagglutinin cleavability and virulence of an avian influenza A virus. J. Virol. **68**:3120–3128.
15. **Iwasaki T, et al.** 2004. Productive infection in the murine central nervous system with avian influenza virus A (H5N1) after intranasal inoculation. Acta Neuropathol. **108**:485–492.
16. **Jang H, et al.** 2009. Highly pathogenic H5N1 influenza virus can enter the central nervous system and induce neuroinflammation and neurodegeneration. Proc. Natl. Acad. Sci. U. S. A. **106**:14063–14068.
17. **Karber G.** 1931. Beitrag zur kollektiven Behandlung pharmakologischer Reihenversuche. Exp. Pathol. Pharmakol. **162**:480–483.
18. **Keawcharoen J, et al.** 2008. Wild ducks as long-distance vectors of highly pathogenic avian influenza virus (H5N1). Emerg. Infect. Dis. **14**:600–607.
19. **Kido H, Okumura Y, Yamada H, Le TQ, Yano M.** 2007. Proteases essential for human influenza virus entry into cells and their inhibitors as potential therapeutic agents. Curr. Pharm. Des. **13**:405–414.
20. **Klenk HD, Garten W.** 1994. Host cell proteases controlling virus pathogenicity. Trends Microbiol. **2**:39–43.
21. **Kuiken T, et al.** 2004. Avian H5N1 influenza in cats. Science **306**:241.
22. **Kuiken T, Taubenberger JK.** 2008. Pathology of human influenza revisited. Vaccine **26**(Suppl 4):D59–D66.
23. **Kuiken T, van den Brand J, van Riel D, Pantin-Jackwood M, Swayne DE.** 2010. Comparative pathology of select agent influenza A virus infections. Vet. Pathol. **47**:893–914.
24. **Lipatov AS, Kwon YK, Pantin-Jackwood MJ, Swayne DE.** 2009. Pathogenesis of H5N1 influenza virus infections in mice and ferret models differs according to respiratory tract or digestive system exposure. J. Infect. Dis. **199**:717–725.
25. **Maines TR, et al.** 2005. Avian influenza (H5N1) viruses isolated from humans in Asia in 2004 exhibit increased virulence in mammals. J. Virol. **79**:11788–11800.
26. **Matsuda K, et al.** 2005. In vitro demonstration of neural transmission of avian influenza A virus. J. Gen. Virol. **86**:1131–1139.
27. **Mori I, Nishiyama Y, Yokochi T, Kimura Y.** 2004. Virus-induced neuronal apoptosis as pathological and protective responses of the host. Rev. Med. Virol. **14**:209–216.
28. **Mori I, Yokochi T, Kimura Y.** 2002. Role of influenza A virus hemagglutinin in neurovirulence for mammalians. Med. Microbiol. Immunol. **191**:1–4.
29. **Munster VJ, et al.** 2009. Pathogenesis and transmission of swine-origin 2009 A(H1N1) influenza virus in ferrets. Science **325**:481–483.
30. **Munster VJ, et al.** Insertion of a multibasic cleavage motif into the hemagglutinin of a low-pathogenic avian influenza H6N1 virus induces a highly pathogenic phenotype. J. Virol. **84**:7953–7960.
31. **Park CH, et al.** 2002. The invasion routes of neurovirulent A/Hong Kong/483/97 (H5N1) influenza virus into the central nervous system after respiratory infection in mice. Arch. Virol. **147**:1425–1436.
32. **Reinacher M, Bonin J, Narayan O, Scholtissek C.** 1983. Pathogenesis of neurovirulent influenza A virus infection in mice. Route of entry of virus into brain determines infection of different populations of cells. Lab. Invest. **49**:686–692.
33. **Reperant LA, Rimmelzwaan GF, Kuiken T.** 2009. Avian influenza viruses in mammals. Rev. Sci. Tech. **28**:137–159.
34. **Schrauwen EJ, et al.** 2011. Insertion of a multibasic cleavage site in the haemagglutinin of human influenza H3N2 virus does not increase pathogenicity in ferrets. J. Gen. Virol. **92**:1410–1415.

35. **Shinya K, et al.** 2011. Subclinical brain injury caused by H5N1 influenza virus infection. J. Virol. **85**:5202–5207.
36. **Shinya K, et al.** 2011. Systemic dissemination of H5N1 influenza A viruses in ferrets and hamsters after direct intragastric inoculation. J. Virol. **85**: 4673–4678.
36a. **Sorrel EM, et al.** 2011. Predicting 'airborne' influenza viruses: (trans-) mission impossible? Curr. Opin. Virol. [Epub ahead of print.] doi: 10.1016/j.coviro.2011.07.003.
37. **Stieneke-Grober A, et al.** 1992. Influenza virus hemagglutinin with multibasic cleavage site is activated by furin, a subtilisin-like endoprotease. EMBO J. **11**:2407–2414.
38. **Swayne DE, Pantin-Jackwood M.** 2006. Pathogenicity of avian influenza viruses in poultry. Dev. Biol. (Basel) **124**:61–67.
39. **Tanaka H, et al.** 2003. Neurotropism of the 1997 Hong Kong H5N1 influenza virus in mice. Vet. Microbiol. **95**:1–13.
40. **van Riel D, et al.** 2010. Seasonal and pandemic human influenza viruses attach better to human upper respiratory tract epithelium than avian influenza viruses. Am. J. Pathol. **176**:1614–1618.
41. **van Riel D, et al.** 2007. Human and avian influenza viruses target different cells in the lower respiratory tract of humans and other mammals. Am. J. Pathol. **171**:1215–1223.
42. **van Riel D, Rimmelzwaan GF, van Amerongen G, Osterhaus AD, Kuiken T.** 2010. Highly pathogenic avian influenza virus H7N7 isolated from a fatal human case causes respiratory disease in cats but does not spread systemically. Am. J. Pathol. **177**:2185–2190.
43. **Webster RG, Bean WJ, Gorman OT, Chambers TM, Kawaoka Y.** 1992. Evolution and ecology of influenza A viruses. Microbiol. Rev. **56**:152–179.
44. **WHO.** 2011, posting date. Confirmed human cases of avian influenza A (H5N1). WHO, Geneva, Switzerland. http://www.who.int/csr/disease/avian_influenza/country/en/index.html.
45. **Zitzow LA, et al.** 2002. Pathogenesis of avian influenza A (H5N1) viruses in ferrets. J. Virol. **76**:4420–4429.